Effect of Contact Force Models on Granular Flow Dynamics

Shunying Ji[1] and Hayley H. Shen, M.ASCE[2]

Abstract: The contact force model consisting of a linear spring dashpot with a frictional glider has been widely adapted to simulate granular flows. Real contact mechanics between two solid bodies is very complicated. Extensive theoretical and experimental studies exist for binary contacts. Very little work has been reported that addresses the effect of contact mechanics on the bulk behavior of granular materials. We first briefly summarize the difference of binary contacts between a linear spring–dashpot model and the Hertzian nonlinear spring with two nonlinear dashpot models. We then compare the constitutive behaviors of a granular material using a linear and a nonlinear model. The stress- and strain-rate relation in simple shear flow and the resulting coordination number are calculated using the discrete element method. It is found that although at the grain level binary contact between two particles depends on whether a linear or a nonlinear model is used, the bulk behavior of granular materials is qualitatively similar with either model.

CE Database subject headings: Models; Granular materials; Solids flow; Stress strain relations.

Introduction

Flows of granular materials have been numerically simulated using disk or sphere particles. Different contact models between particles may be applied to obtain the dynamic interaction between the stress and strain rate. The most widely used is the linear spring–dashpot model with a frictional limit in the tangential direction (e.g., Cundall et al. 1979; Zhang and Rauenzahn 2000; Campbell 2002). In fact, contact mechanics between solid surfaces is a complex subject that has been studied for over a century. The seminal work of Hertz (1882) for elastic spheres is one example. Theoretical development for idealized cases is summarized in Johnson (1987).

Linear spring dashpot is a drastic simplification of the real contact between objects. Numerous different models and their implications in the force–velocity–displacement relation between two contacting objects have been discussed in the literature (e.g., Zhang and Whiten 1996; Kuo et al. 2002; Mishra and Murty 2001; Roux 2004; Di Maio and Di Renzo 2004a,b). Some of these models focused on the end results of the energy dissipation represented by the restitution coefficient (Ramirez et al. 1999); some focused on the micromechanics at the contact surface resulting in local slip and plasticity (Vu-Quoc et al. 2001). Thermodynamic inconsistency has been shown in some simplified contact models (Elata and Berryman 1996).

To numerically simulate a large number of interacting par-ticles, a simple algorithm is desired. Therefore, the linear contact model has its appeal. The key question is: Does the contact model affect the bulk behavior of a granular material? Surprisingly, not much has been reported concerning this issue. Mishra and Murty (2001) compared the results between a linear and a nonlinear contact model applied to a ball mill. They found that if one chose the parameters in the linear model by minimizing the difference between the contact forces over the whole duration of impact, the power requirement for the ball mill from the two models is almost the same.

In this study, we investigate a subset of a general power-law contact model that includes both the linear and the Hertz contact models. We first examine the binary collision properties: force–velocity–displacement relation and the velocity-dependent restitution. We then investigate the bulk behavior represented by the stress–strain-rate relation and the coordination number. The effect of linear versus nonlinear contact models will be observed. A discrete element simulation of nonuniform particles in a simple shear flow generates the data for this study.

Linear and Nonlinear Contact Models for Normal Collisions

In this section we consider the impact of the contact force model on binary collisions. To simplify the analysis, we concentrate on the normal impact only. A great many studies have been performed on particle collisions with physical experiments and theoretical analysis (e.g., Bridges et al. 1984; Zhang and Whiten 1996; Ramirez et al. 1999; Mishra and Murty 2001; Di Maio and Di Renzo 2004a,b). Here, a brief review of some key studies relevant to this work will be given.

The contact force between two particles is most commonly described with an elastic spring and a viscous dashpot. The following represents a general model (Ramirez et al. 1999)

$$m\ddot{x} = F_e + F_v; \quad F_e = K_n x^\alpha \quad \text{and} \quad F_v = C_n x^\beta \dot{x} \quad (1)$$

where m=particle mass; K_n and C_n=effective stiffness and viscosity, respectively; x represents the amount of overlap between

[1]Associate Professor, State Key Laboratory of Structural Analysis for Industrial Equipment, Dalian Univ. of Technology, Dalian 116023, China.

[2]Professor, Dept. of Civil and Environmental Engineering, Clarkson Univ., Potsdam, NY 13699-5710 (corresponding author). Email: hhshen@clarkson.edu

the two particles; and $\dot{x}$=relative velocity of the two particles moving towards each other. When $\alpha=1$, $\beta=0$ the above is the usual linear spring–dashpot case. The Hertz contact model is realized when $\alpha=3/2$, $C_n=0$.

In the linear contact force model, the viscous coefficient

$$C_n^L = \zeta_n \sqrt{2MK_n^L} \qquad (2)$$

where M=mean mass of the two colliding particles; K_n^L and C_n^L=effective viscous coefficient and stiffness of the linear contact model; and ζ_n is related to the restitution coefficient e through (Babic et al. 1990)

$$\zeta_n = \frac{-\ln e}{\sqrt{\pi^2 + \ln^2 e}} \qquad (3)$$

Since $F_v = C_n^L \dot{x}$ in a linear spring–dashpot model, the initial impact force is not zero despite the absence of particle overlap. Zhang and Whiten (1996) and several other investigators pointed out this problem in a linear model. For any nonlinear (NL) damping such that $F_V = C_n^{NL} x^\beta \dot{x}$, the initial damping force vanishes with any positive β. Both the linear and nonlinear models predict force reversal at the end of an impact (Zhang and Whiten 1996; Kuo et al. 2002). Such spurious attractive force should not be present for cohesionless materials, indicating the nonphysical behavior of the viscous damping in general.

From the Hertz theory, the normal stiffness coefficient for an elastic sphere may be written as

$$K_n^{NL} = \frac{\sqrt{2}}{3} \frac{E\sqrt{R}}{(1-\nu^2)} \qquad (4)$$

where K_n^{NL}=stiffness of nonlinear contact model; R=particle radius; and E and ν=Young's modulus and Poisson ratio of the particle, respectively. The above nonlinear model has been compared favorably to physical experiments and numerical solutions (Falcon et al. 1998; Zhang and Whiten 1996).

For elastic spheres, $\alpha=3/2$ has been well established. On the other hand, at least two different values for β have been found based on experimental data and analytical solutions. Kuwabara and Kono (1987) extended the Hertz theory, and found that $\beta=1/2$ for a sphere-to-sphere contact. This value of β was verified for steel ball impact on a steel rod (Mishra and Murty 2001). Experiments by Falcon et al. (1998) using tungsten carbide impacting on a flat duralumin plate showed that it was better to set $\beta=1/4$. Briggs and Bearman (1995) conducted an experiment using several types of rocks including sandstone, granite, and basalt. Their data also suggested $\beta=1/4$. Zhang and Whiten (1996) used a dimensional argument to suggest $\beta=1/4$ for Hertzian contacts. From these studies, it is clear that different materials may require different nonlinear models to accurately describe their contact mechanics. In the subsequent analysis, we will study $\alpha=1$ with $\beta=0$ and $\alpha=3/2$ with $\beta=1/4$ or $\beta=1/2$.

Numerical Simulation of Two Particles in a Normal Collision

In this section, we will study the difference between linear and nonlinear models in a binary collision using a numerical procedure. We compare the resulting force, displacement (overlap), and relative velocity during two particles engaged in a normal collision and the relationship between the initial velocity and the restitution coefficient. For special cases these results have been obtained analytically. The numerical approach provides a tool for cases in which analytical solutions are not possible.

For the linear model, we set the effective stiffness $K_n^L = 1 \times 10^4$ N/m, particle diameter $D=1$ cm, and density $\rho = 1 \times 10^3$ kg/m^3. There is no standard way to establish a quantitative comparison between different contact models. In order to facilitate a qualitative comparison among different contact models, our strategy is to first define a maximum displacement (overlap) from the collision, then choose the nonlinear spring constant so that the maximum elastic force is the same in both the linear and nonlinear models. Using this spring constant, we determine the damping parameters so that the restitution coefficients are the same in the corresponding models. However, as will be shown below, the restitution coefficient could be dependent on impact velocity in some nonlinear models. In this case, we fix an initial velocity to continue the comparison. In what follows, we will investigate the range of restitution coefficient from 1.0 to 0.1.

Using the set of parameters described, Eq. (1) is solved numerically with initial velocity $v_0=0.6$ m/s, to obtain the particle overlap, force, and relative velocity. The results simulated with a linear contact model are obtained first. The maximum overlap of an elastic contact with $e=1$ for the set of parameters chosen is about 0.1 mm, or 1% of the particle diameter. To obtain the same elastic force under this maximum overlap with nonlinear models, we need $K_n^L x_{max} = K_n^{NL} x_{max}^{3/2}$, where x_{max}=maximum overlap; and K_n^L and K_n^{NL}=stiffness coefficients in linear and nonlinear contact models, respectively. With $K_n^L = 1 \times 10^4$ N/m, $x_{max}=0.1$ mm in the linear model, the "equivalent" stiffness of nonlinear models is $K_n^{NL} = 1 \times 10^6$ N/m$^{3/2}$ when $\beta=1/4$ or $1/2$. The corresponding damping coefficient C_n for the linear contact model may be calculated using Eqs. (2) and (3). The elastic and viscous forces interact in the nonlinear models. No analytic relation exists between the restitution and damping coefficient. Therefore, we numerically solve for the restitution under different C_n and choose the corresponding values required to match the linear case.

In the numerical simulation of the linear contact model, the computational time step is normally set as 1/50 of the binary contact time (Campbell 2002; Shen and Sankaran 2004). In the nonlinear model, the computational time step cannot exceed the Rayleigh time

$$T_R = \frac{\pi R}{0.16\nu + 0.88} \sqrt{\rho/G}$$

where R=particle radius; and G=shear modulus. The Rayleigh time is the time required for a Rayleigh wave to travel the diameter of an elastic particle. For computational stability, the time step has to be smaller than the Rayleigh time as well as the characteristic time of the system dynamics determined by the fastest moving and the smallest particles (Kremmer and Favier 2001). Since the Rayleigh time is proportional to the binary contact time (Babic et al. 1990), in this study we use a more conservative value and let the time step be identical in both the linear and nonlinear models. The total computational times for both models are, therefore, very similar.

Results of the overlap, contact force, and relative velocity between two contacting particles are given in Fig. 1. These results show that for a pure elastic collision, $e=1$, the particle overlap and the interparticle force increase from zero to the maximum, then symmetrically decrease to zero for both linear and nonlinear models. But for dissipative collisions, differences exist among
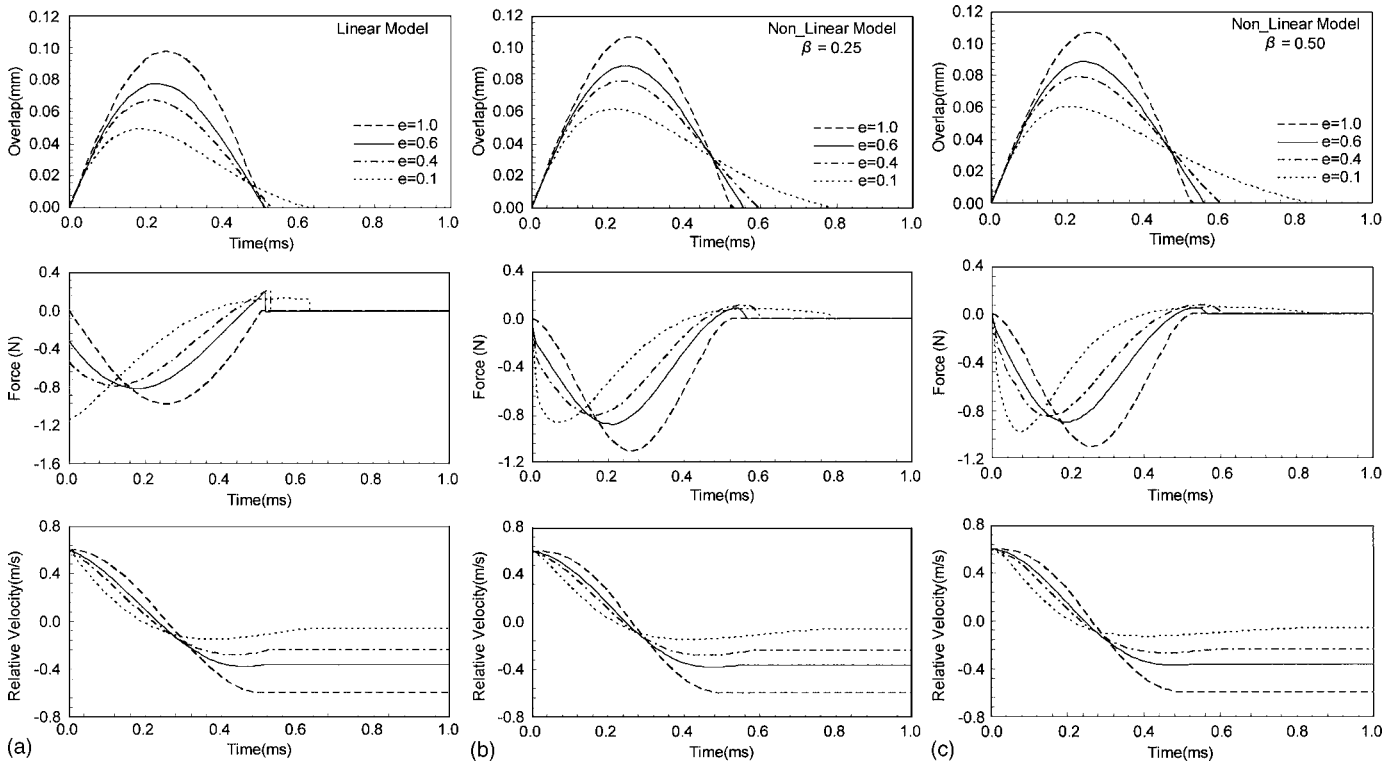
Fig. 1. Comparisons between linear and nonlinear models for particle–particle collision

linear and nonlinear models. In the linear model, the initial contact force is not zero due to the simple viscous model, while the nonlinear models are more reasonable, as pointed out in several previous studies (e.g., Zhang and Whiten 1996). The contact duration is sensitive to the choice of linear or nonlinear models. These results are identical to those obtained analytically for the linear contact model and nonlinear model when $\beta=1/4$ (Zhang and Whiten 1996; Kuo et al. 2002). Just as previously reported, spurious force reversal towards the end of the collision is observed in all cases except when $e=1$.

It is well known that the restitution coefficient e depends on the impact velocity. Ramirez et al. (1999) obtained a velocity-dependent analytical solution of the restitution coefficient based on Eq. (1). In their study, the dimensionless equation of motion for colliding particles can be written as

$$\ddot{\hat{x}} + \delta(v)\hat{x}^{\beta}\dot{\hat{x}} + \frac{1+\alpha}{2}\hat{x}^{\alpha} = 0, \quad \delta(v) = C_n \left(\frac{1+\alpha}{2K_n} \right)^{\frac{1+\beta}{1+\alpha}} v^{[2(\beta-\alpha)/(1+\alpha)]+1}$$

(5)

where the dimensionless variables are defined as $\hat{x}=x/x_0$, $\dot{\hat{x}}=\dot{x}/v$ and $\ddot{\hat{x}}=(x_0/v^2)\ddot{x}$, in which

$$x_0 = \left(\frac{\alpha+1}{2K_n} \right)^{\frac{1}{1+\alpha}} v^{\frac{2}{1+\alpha}}$$

and v=initial velocity. With the initial and terminal conditions $\hat{x}(0)=0$, $\dot{\hat{x}}(0)=1$, $\hat{x}(t_c)=0$, and $\dot{\hat{x}}(t_c)=-e$, t_c=dimensionless duration of the collision, the solution of Eq. (5) is completely determined. Ramirez et al. (1999) thus proved that the dependence of the terminal velocity on the initial velocity is entirely through the parameter $\delta(v)$. Therefore, when the power of v in $\delta(v)$ vanishes the restitution coefficient does not depend on the initial velocity. For the power to vanish

$$2(\beta - \alpha) + (1 + \alpha) = 0$$

(6)

The following two special cases satisfy the above equation: (i) a linear model where $\alpha=1$ and $\beta=0$ and (ii) the Hertz contact law $\alpha=3/2$, and a viscous model with $\beta=1/4$.

If $\alpha=3/2$ and $\beta=1/2$, the normal restitution coefficient will dependent on the impact velocity. For this nonlinear model, the elastic force is based on the Hertz contact law, and the dissipative force (viscous force) is calculated as (Schager and Poschel 1998; Ramirez et al. 1999)

$$F_v = \frac{3}{2}AK_n\sqrt{x}\dot{x}$$

(7)

where

$$A = \frac{1}{3} \frac{(3c_2 - c_1)^2}{3c_2 + 2c_1} \frac{(1 - v^2)(1 - 2v)}{Ev^2}$$

c_1 and c_2=damping coefficients of the pair of impacting particles. Ramirez et al. (1999) obtained an analytic solution for the restitution coefficient in terms of the following power series:

$$e_n = 1 + a_1 \left(\frac{v}{v^*} \right)^{1/5} + a_2 \left(\frac{v}{v^*} \right)^{2/5} + a_3 \left(\frac{v}{v^*} \right)^{3/5} + a_4 \left(\frac{v}{v^*} \right)^{4/5} \cdots$$

(8)

with $a_1=-1$, $a_2=3/5$, $a_3=-0.315119$, $a_4=0.161167$, and $(v^*)^{-1/5}$ $=1.15344[(3/2)A][(K_n/M_e)]^{2/5}$ where $M_e=(M_A M_B)/(M_A+M_B)$ =effective mass of two particles M_A and M_B.

Bridges et al. (1984) measured the normal restitution coefficient with ice particles under different impact velocities, and found that the normal restitution coefficient could be fitted with
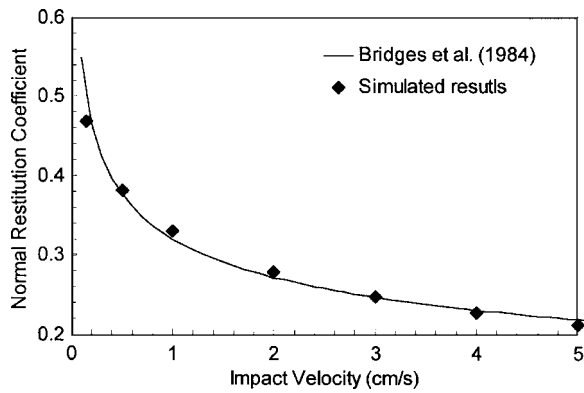
Fig. 2. Dependence of normal restitution on impact velocity for ice particles

$$e = 0.32v^{-0.234} \qquad (9)$$

This empirical formula appears to be quite different from Eq. (8). To test this, we integrate Eq. (5) numerically with $\alpha=3/2$, $\beta=1/2$ to determine the restitution coefficient. Basically, we bypassed the analytic solution by directly simulating the restitution using the same contact law as in Ramirez et al. (1999). In the numerical simulation, we use the appropriate parameters for ice particles: $E=9.1$ GPa, $\nu=0.28$, $\rho=920$ kg/m^3, and set $D=0.01$ m. The coefficient A in Ramirez et al. (1999) is considered here as a fitting parameter due to the lack of information of c_1 and c_2. We set $A=2.35E-5$. Eq. (9) from Bridges et al. (1984) and the present numerical reproduction of Ramirez's results compared well, as shown in Fig. 2. Thus Eq. (8) predicts similar results as the empirical formula Eq. (9) suggested in Bridges et al. (1984).

Granular Flow Dynamics Simulated with Linear and Nonlinear Models

So far, we have witnessed that contact law affects the details of the force–velocity–displacement relation between two impacting particles. Both the linear and nonlinear viscoelastic models have problems describing the real physics of particle collisions. We have also observed that contact law influences the dependence of energy dissipation on the initial impact velocity. Next, we studied the effect of contact law on the bulk behavior of granular flows using the numerical procedure described in the binary collision above. In particular, we focused the stress–strain-rate relation, the coordination number, and the contact time of a simple shear flow of multisize spheres.

We studied a system of spherical particles with a narrow size distribution. The maximum and minimum particle sizes are $D_{min}=0.9D$ and $D_{max}=1.1D$, respectively. Here, $D=$mean particle diameter. We use a discrete element simulation to study the simple shear flow of such a system. To create a simple shear system with a finite number of particles, periodic boundary conditions were applied. The computational domain is $10D \times 10D \times 10D$. The particles are initially randomly placed in this domain. The mean particle size is set at $D=1$ cm, particle density $\rho=1\times 10^3$ kg/m^3, and the contact friction coefficient is set at $\mu=0$ in order to concentrate on the elastic and viscous effects. For the linear model, the effective normal stiffness is set at $K_n^L=1.0\times 10^4$ N/m, and restitution coefficient $e=0.6$, corresponding to damping coefficient $C_n=0.52$ N s/m. In the

Table 1. Relationship between Restitution and Damping Coefficients in Contact Models

Material parameter	Case 1	Case 2	Case 3	Case 4
Restitution coefficient e	1.00	0.60	0.40	0.10
C_n (Ns/m) in linear model	0.00	0.52	0.91	1.91
C_n (Ns/m$^{5/4}$) in non-linear model with $\beta=1/4$	0.00	5.80	10.13	21.39
C_n (Ns/m$^{3/2}$) in non-linear model with $\beta=1/2$[a]	0.00	75.26	134.09	315.65

[a]v_0 is set as 0.6 m/s for this case.

nonlinear model, $\alpha=3/2$, and $\beta=1/2$ or $1/4$. With the same particle size, density, and stiffness as in Fig. 1, the normal stiffness for the nonlinear case is set at $K_n^{NL}=1.0\times 10^6$ N/m$^{3/2}$. The damping coefficients for the nonlinear cases are from Table 1, i.e., $C_n=5.80$ N s/m$^{5/4}$ for $\beta=1/4$, and $C_n=75.26$ N s/m$^{3/2}$ for $\beta=1/2$. Because we study the frictionless case, the tangential stiffness has no effect. Other details of the simulation follow those described in Babic et al. (1990) and Shen and Sankaran (2004), except the code is now expanded to simulate three-dimensional (3D) spherical particle systems.

The dimensionless stress $\tau_{ij}^*=\tau_{ij}/\rho D^2 \dot{\gamma}^2$ and dimensionless shear rate $S=\dot{\gamma}\sqrt{\rho D^3/K_n}$ are used to analyze the relationship between stress and shear rate. Here, the "equivalent" stiffness of linear model $K_n^L=1.0\times 10^4$ N/m is adapted in the dimensionless shear rate for all three contact models. Using the parameters above, four quantities are plotted in Figs. 3–5: the dimensionless shear and normal stresses, and the coordination number and the mean contact time with linear and nonlinear models. Only steady-state data are presented in Figs. 3–5. The simulations were performed until the strain became 50. The stress curves were checked to confirm steady state. In the stress components, x indicates the direction of shear and y the direction of shear gradient. Fig. 3 is the summary of the linear case, where the resulting dimensionless shear and normal stress, coordination number, and contact duration are plotted. Fig. 4 summarizes the first nonlinear case where $\alpha=3/2$, $\beta=1/4$, and Fig. 5 is for the second nonlinear case where $\alpha=3/2$, $\beta=1/2$. We investigate a range of particle concentrations from 0.4 to 0.65, and a range of dimensionless shear rates from 10^{-3} to $10^{-1/2}$.

First, we compare the general appearance of the corresponding plots among the three contact models. The range of dimensionless stresses: shear and normal, coordination number, and contact time duration, are very similar from one model to another. In a log–log plot, only order of magnitude differences are immediately visible. Therefore, when we compare these results among different contact models, we notice that they do differ quantitatively, but are within the same order of magnitude for the four quantities plotted.

The first two of the plots in Figs. 3–5 are the dimensionless stresses. At low concentrations these dimensionless stresses do not depend on the shear rate until dimensionless shear rate S exceeds 0.1. When the concentration becomes greater than 0.62, the dimensionless stresses in the log–log plot have a slope of -1, indicating the real stresses become independent of the shear rate. This same behavior was discussed in Babic et al. (1990) for two-dimensional (2D) assembly of uniform disks and in Campbell (2002) for 3D assembly of uniform spheres. This "phase transition" is extensively discussed in Campbell (2002). In his work, Campbell suggests that the strength of the force chains developed in the granular shear flow is responsible for the transition from a rate-dependent constitutive relation to a rate-independent case. Comparing these first two plots in each of Figs. 3–5, it is ob-
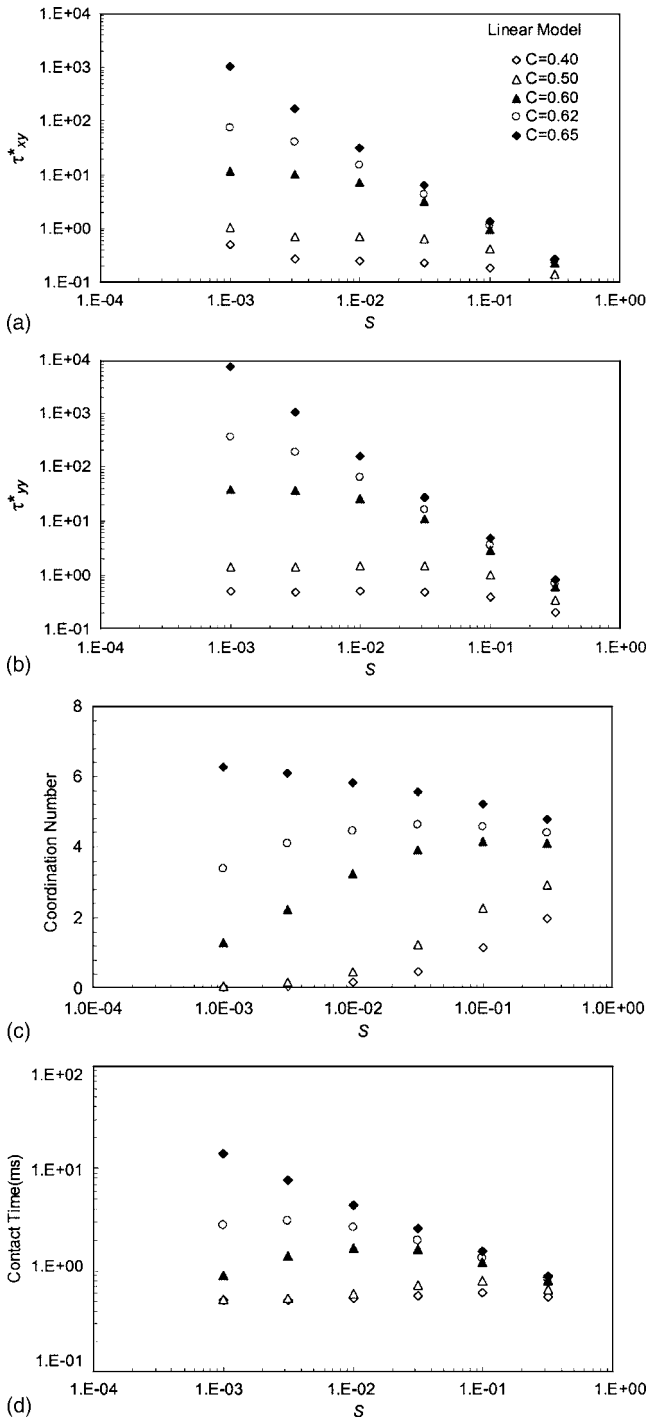
Fig. 3. Bulk behavior of granular shear flow simulated with linear model

Fig. 4. Bulk behavior of granular shear flow simulated with nonlinear model ($\beta = 1/4$)

served that such a transition is independent of the contact model. We may also add that such a transition is independent of whether uniform size particles or, in this case, a narrow size distribution of particles, are investigated.

In the present discrete element method simulations we covered a very wide range of flow states. The corresponding particle deformation could be significant. If we use the linear contact model, the relative mean deformation h can be estimated with $(h/D) \sim (\tau_{yy}D/K_n) = S^2 \tau_{yy}^*$. Using this estimation, from Fig. 3 it can be found that large deformations in excess of 1.0×10^{-2} occur in some of the cases. Most of the natural granular materials are
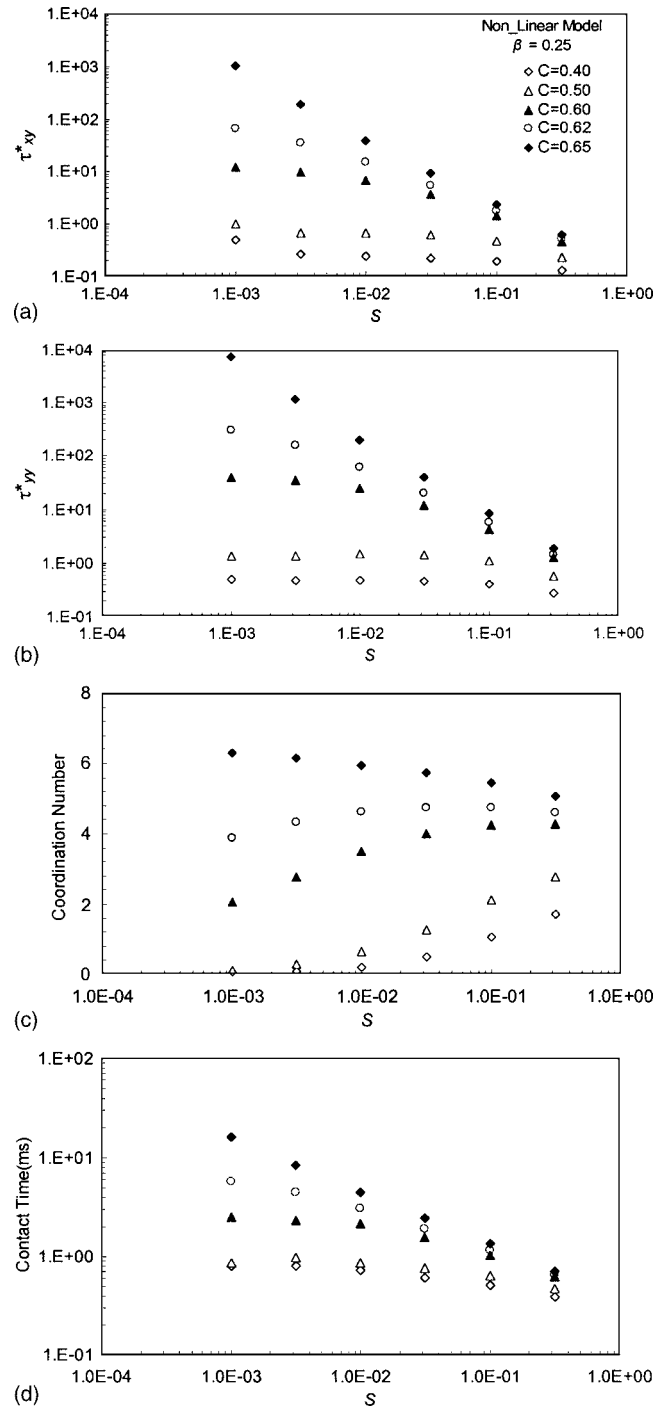
rigid enough so that such large overlaps are uncommon. But, manufactured granular materials of softer nature can reach such deformation under an ordinary load.

If we further examine the coordination number, we observe that a distinct change of behavior occurs when the concentration increases. When the concentration is below 0.62, the coordination number increases with increasing shear rate. The reverse is true for concentrations of 0.65. This clear demarcation between rate-dependent and rate-independent constitutive relations that is observed in the stresses is, again, the same for all contact models studied here.
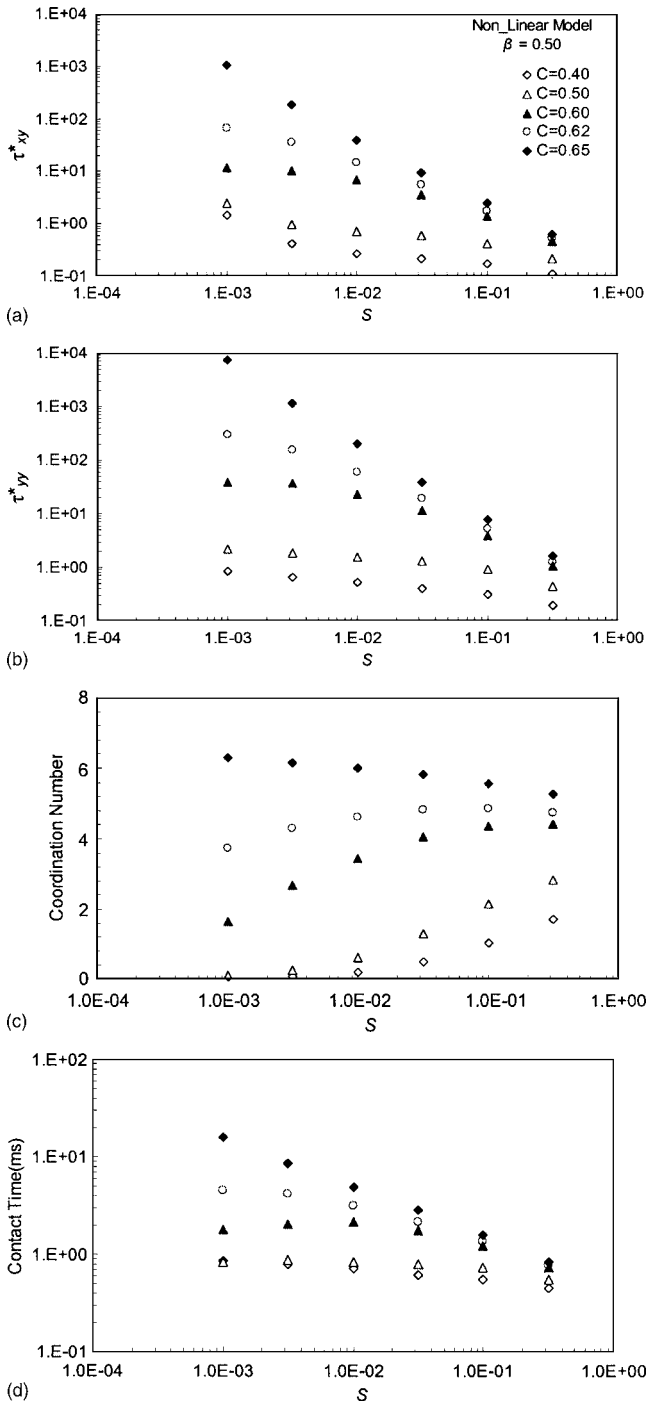
Fig. 5. Bulk behavior of granular shear flow simulated with nonlinear model ($\beta = 1/2$)

Fig. 6. Bulk friction versus inertia number

The third plot of Figs. 3–5 is to show the mean contact duration between particles. This is a measure of the possibility to form groups of simultaneously colliding particles or the stability of the force chains, if any, established in the assembly (Zhang and Rauenzahn 2000; Shen and Sankaran 2004). The contact duration decreases with increasing shear rate in all cases. This agrees with intuition, since the more dynamic the shearing is the more likely contacts can be built, but also more likely they can be terminated. Therefore, we expect the force chains to weaken as the shear rate increases. At very low concentrations, 0.4 and 0.5, the contact time becomes nearly independent of the shear rate. At these

low concentrations, the coordination number indicates that most of the collisions are binary; no force chains exist. Since the duration of the contact time is independent of the collisional velocity in a linear model and only weakly dependent on the velocity in a nonlinear model from our numerical results for Eq. (1), it is natural to expect a near-constant contact duration for low concentrations.

Discussion

Two recent studies considered Couette type 2D planar dense granular flows (MiDi 2004; da Cruz et al. 2005), in which the resulting bulk friction was related to the inertial number defined as $I = \dot{\gamma} D \sqrt{\rho_g / \sigma_{yy}}$, here ρ_g = bulk density. It was found that the bulk friction of a granular material over a large range of shear rate and solid concentration collapses onto a single curve in terms of I. Using the current data for a simple shear flow, we test whether a similar trend holds. Figs. 6 and 7 are re-plots of the same data as in Figs. 3–5. Unlike in MiDi (2004) and da Cruz et al. (2005), we group the data into different dimensionless shear rates. In this
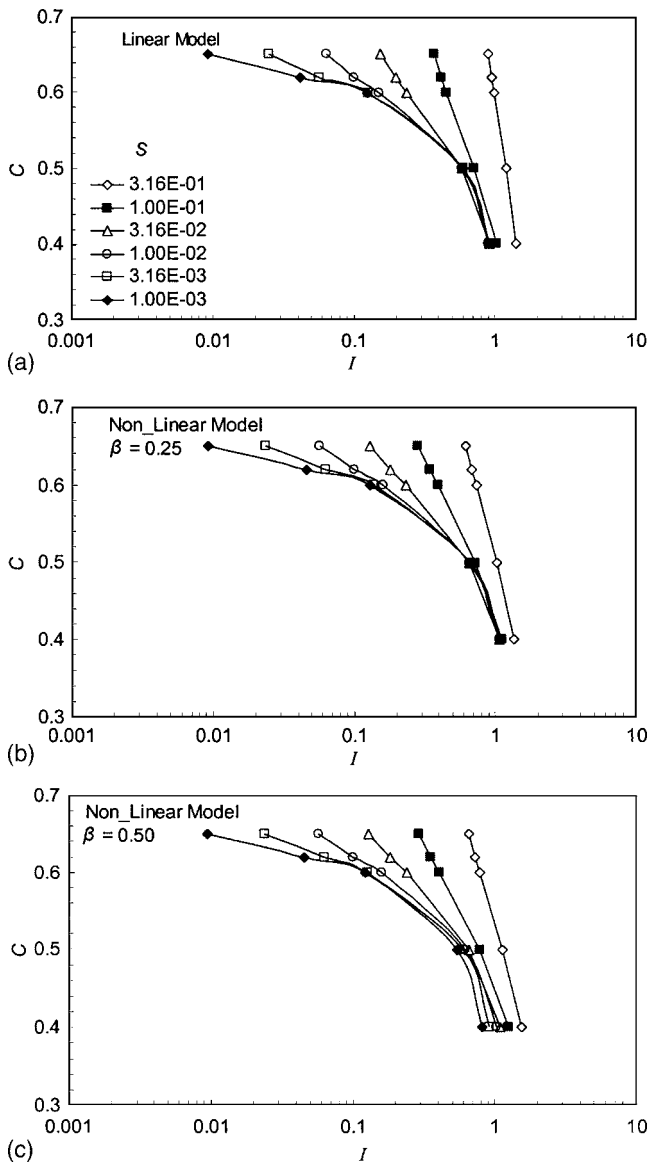
Fig. 7. Concentration versus inertia number

bulk behavior of granular materials does not appear to be sensitive to the contact model, at least qualitatively.

In other numerical studies of granular materials using linear and nonlinear contact force models, a similar conclusion was also obtained. For example, in the numerical study of granular packings, the probability distribution of contact forces calculated with linear and nonlinear contact force models are compared (Silbert et al. 2002). In a 2D annulus shear test simulated with linear and nonlinear contact force models, the calculated porosities of multisize disk-shaped granular materials are also very close (Claquin and Emeriault 2004).

Conclusions

In this study we adapt a simple general contact law with a parallel spring and dashpot element. Both linear and Hertz nonlinear models are included in this general model with three damping choices: one linear and two nonlinear. To compare these three models, the collision processes between two particles are first summarized. Then, the bulk behaviors of granular materials under a simple shear motion are simulated. From the result of this study, contact mechanics does play an important role at the binary collision level, both quantitatively and qualitatively, but the linear contact model is sufficient to describe qualitatively the bulk behavior of granular materials. Quantitatively, results from a linear contact model are different from nonlinear models. Within the nonlinear models, results can be different for different model parameters. Further study is required to determine the extent of these differences, especially for frictional materials.

Acknowledgments

way, more details of the bulk friction behavior in relation to I are found. In general, the trend of increasing bulk friction and decreasing concentration with increasing I are the same as those previously found for a 2D Couette-type flow. Such a trend is not affected by whether a linear or a nonlinear contact model is used. Because of the difference in material parameters used, quantitative comparisons are not possible. Here, we used $e=0.6$, $\mu=0$ while MiDi (2004) used $e=0.1$ or 0.9, $\mu=0$, and 0.1–0.8, da Cruz et al. (2005) used $e=0.1$ or 0.9, $\mu=0.0$, 0.4, and 0.8. However, it is interesting to note that the bulk friction at low I approaches 0.1 for the $\mu=0$ case, the same as in Midi (2004) and da Cruz et al. (2005) despite the difference in other material parameters. By grouping the results into different dimensionless shear rates, we find that shear rate does play a role in the bulk behavior in addition to I. This dependence weakens as the solid concentration decreases, as is clearly seen in Fig. 7.

As shown in Figs. 6 and 7, the stress levels, their dependence on the shear rate, the coordination number variations, and the contact duration are all qualitatively the same among the three contact models. Therefore, in the simple shear granular flow the

References

Babic, M., Shen, H. H., and Shen, H. T. (1990). "The stress tensor in granular shear flows of uniform deformable disks at high solids concentrations." *J. Fluid Mech.*, 219, 81–118.

Bridges, F. G., Hatzes, A. P., and Lin, D. N. C. (1984). "Structures, stability, and evolution of Saturn's rings." *Nature (London)*, 309, 333–335.

Briggs, C., and Bearman, R. (1995). "The assessment of rock breakage and damage in crushing machinery." *Proc., EXPLO'95*, Brisbane, Australia, l67.

Campbell, C. (2002). "Granular shear flows at the elastic limit." *J. Fluid Mech.*, 465, 261–291.

Claquin, C., and Emeriault, F. (2002). "Interface behavior of granular materials: Discrete numerical simulation of a ring simple shear test." *Proc., 15th ASCE Engineering Mechanics Conf.*, Columbia Univ., New York.

Cundall, P., and Strack, O. (1979). "A discrete numerical model for granular assemblies." *Geotechnique*, 29, 47–65.

da Cruz, F., Eman, S., Prochnow, M., Roux, J.-N., and Chevoir, F. (2005). "Rheophysics of dense granular materials: Discrete simulation of plane shear flows." *Phys. Rev. E*, 72, 021309.

Di Maio, F. P., and Di Renzo, A. (2004a). "Analytical solution for the problem of frictional–elastic collisions of spherical particles using

the linear model." *Chem. Eng. Sci.*, 59, 3461–3475.

Di Maio, F. P., and Di Renzo, A. (2004b). "Comparison of contact-force models for the simulation of collisions in DEM-based granular flow codes." *Chem. Eng. Sci.*, 59, 525–541.

Elata, D., and Berryman, J. G. (1996). "Contact fore-displacement laws and the mechanical behavior of random packs of identical spheres." *Mech. Mater.*, 24, 229–240.

Falcon, E., Laroche, C., Fauve, S., and Coste, C. (1998). "Behavior of an elastic ball bouncing repeatedly off the ground." *Eur. Phys. J. B*, 3, 45–57.

Hertz, H. (1882). "Uber die beruhrung fester elasticcher korper (On the contact of elastic solids)." *J. Reine Angew. Math.*, 92, 156–l71.

Johnson, K. L. (1987). *Contact mechanics*, Cambridge Univ. Press, Cambridge, U.K.

Kremmer, M., and Favier, J. F. (2001). "A method for representing boundaries in discrete element modeling. Part II: Kinematics." *Int. J. Numer. Methods Eng.*, 51, 1423–1436.

Kuo, H. P., Knight, P. C., Parker, D. J., Tsuji, Y., Adams, M. J., and Seville, J. P. K. (2002). "The influence of DEM simulation parameters on the particle behavior in a V-mixer." *Chem. Eng. Sci.*, 57, 3621–3638.

Kuwabara, G., and Kono, K. (1987). "Restitution coefficient in a collision between two spheres." *Jpn. J. Appl. Phys., Part 1*, 26(8), 1230–1233.

MiDi, G. D. R. (2004). "On dense granular flows." *Eur. Phys. J. E*, 14, 341–365.

Mishra, B. K., and Murty, C. V. R. (2001). "On the determination of contact parameters for realistic DEM simulations of ball mills." *Powder Technol.*, 115, 290–297.

Ramirez, R., Poschel, T., Brilliantov, N. V., and Schwager, T. (1999). "Coefficient of restitution of colliding viscoelastic sphere." *Phys. Rev. E*, 60(4), 4465–4472.

Roux, J.-N. (2004). "Elasticity, quasistatic deformation, and internal state of sphere packings." *Proc., 17th ASCE Engineering Mechanics Conf.*, Univ. of Delaware, Newark, Del.

Schager, T., and Poschel, T. (1998). "Coefficient of restitution of viscous particles and cooling rate of granular gases." *Phys. Rev. E*, 57(1), 650–654.

Shen, H. H., and Sankaran, B. (2004). "Internal length and time scales in a simple shear granular flow." *Phys. Rev. E*, 70(5), 051308.

Silbert, L. E., Grest, G. S., and Landry, J. W. (2002). "Statistics of the contact network in frictional and frictionless granular packings." *Phys. Rev. E*, 65, 061303.

Vu-Quoc, L., Zhang, X., and Lesburg, L. (2001). "Normal and tangential force-displacement relations for frictional elastoplastic contact of spheres." *Int. J. Solids Struct.*, 38, 6455–6489.

Zhang, D., and Whiten, W. J. (1996). "The calculation of contact forces between particles using spring and damping models." *Powder Technol.*, 88, 59–64.

Zhang, D. Z., and Rauenzahn, R. M. (2000). "Stress relaxation in dense and slow granular flows." *J. Rheol.*, 44(5), 1019–1041.